PERFORMANCE TESTING OF ADVANCED LEAD–ACID BATTERIES FOR ELECTRIC VEHICLES

B. K. MAHATO, G. H. BRILMYER and K. R. BULLOCK

Corporate Applied Research, Johnson Controls, Inc., P.O. Box 591, 5757 North Green Bay Avenue, Milwaukee, WI 53201 (U.S.A.)

The program established by the United States Department of Energy through Argonne National Laboratory for development of lead–acid batteries for electric vehicles consisted of two phases. The first phase was a 3-year effort to develop an Improved State of the Art (ISOA) electric vehicle battery. The performance testing of 2 sizes of ISOA batteries developed by Johnson Controls, Inc., the EV2300 and the EV3000, is described elsewhere [1].

In the second phase of the program, the goals shown in Table 1 for an Advanced lead–acid battery were established [2]. This paper describes the performance testing of one Advanced battery design developed by Johnson Controls, Inc., which was designed to meet the 1983 goals.

TABLE 1

DOE goals — Advanced lead–acid battery

	1983	1986
Specific energy (W h kg^{-1}) (3 h rate to 1.75 V/cell)	45	56
Vol. energy density (W h l^{-1})	100	120
Specific power (W kg^{-1}) (30 s avg. at 50% DOD to 1.4 V/cell)	104	104
Energy efficiency	>75%	>75%
Life (at 80% DOD)	650 cycles	800 cycles

This Advanced battery is the same size as the EV3000 ISOA battery, 38.1 cm long × 33.0 cm wide × 29.5 cm high. The weight of this Advanced design is 75.0 kg for a 12 V module with acid circulation subsystem included, compared with 73.1 kg for the EV3000. The Advanced design incorporates all the features of the ISOA battery, which are summarized in Table 2 [1]. The major change from the ISOA EV3000 design in the Advanced design is the use of 15 rather than 11 electrodes per cell. The

TABLE 2

ISOA and Advanced battery design features

1. Thin-walled polypropylene case [5]
2. Low resistance intracell welds [6]
3. Glass mat and microporous polyethylene envelope separator [7]
4. Radial grid design [7 - 9]
5. Electrolyte circulation subsystem [2, 7, 8, 10 - 14]
6. Semiautomatic venting and watering subsystem [2]
7. Thermal management subsystem [14, 15]
8. Programmable charger for overcharge control [14]

Advanced design gives increased material utilization by increasing the plate surface area and decreasing the plate thickness.

The tests were run on single cells equipped with an acid circulation subsystem and reference electrodes. The cyclers and data acquisition system, which have previously been described [3], are designed to monitor cell voltages and currents, half-cell potentials, charge and discharge times, and temperature. Capacities and energies are calculated automatically and can be corrected for temperature.

Data on the effect of discharge rate on the cell capacity were obtained from 3 cells which were first cycled using a constant current, 83 A discharge to 1.75 V for 20 - 38 cycles until their capacities were well established. At this rate the capacities of the 3 cells were nearly identical. The cells were subsequently discharged at the 3, 4.5 and 9 hour rates.

Peukert plots for the Advanced battery and the EV3000 are shown in Fig. 1. According to Peukert's empirical equation [4],

$$\log t = \log C - n \log i,$$

where t is the discharge time in hours, i is the discharge current in amps and n and C are constants which are characteristic of the battery design. Therefore, for a constant current discharge, a log–log plot of the discharge time *versus* discharge current is a straight line of slope $-n$ and intercept, log C. Values of n and log C of 1.20 and 2.83, respectively, for the Advanced cell design were determined with a least-squares-fit of the straight line. The correlation coefficient was 0.988. These values compare with n and log C values of 1.28 and 2.91, respectively, for the EV3000 [1]. The Advanced cell design has a higher capacity at all currents tested. The capacity difference between the two designs increases as the discharge current increases, as indicated by the lower n value for the Advanced design. Since the Advanced cell has thinner plates and higher surface area, its high rate performance is better.

Table 3 shows the energies and powers, currents and average cell voltages for 10 cells made over about a 3 year period. Values for W h kg^{-1} and W kg^{-1} were calculated for a 6-cell battery module by multiplying the single cell values for energy and power by 6 and dividing by the module

TABLE 3

Performance of Advanced cell design between 20 and 40 cycles

No. of cells tested	Discharge rate (A)	Mean cell voltage (V) (1σ)	Energy (W h) (1σ)	Power (W) (1σ)	Specific energy (W h kg^{-1})	Specific power (W kg^{-1})
1	35.0	1.975	651.5	69.1	52.1	5.53
1	41.5	1.983	635.0	82.2	50.8	6.58
1	65.0	1.950	541.4	126.7	43.3	10.1
10	83.3	1.957(0.0117)	562.7(20.88)	163.0(1.01)	45.0	13.0
2	94.0	1.944	506.9	182.7	40.6	14.6
1	124.5	1.915	485.0	238.5	38.8	19.1

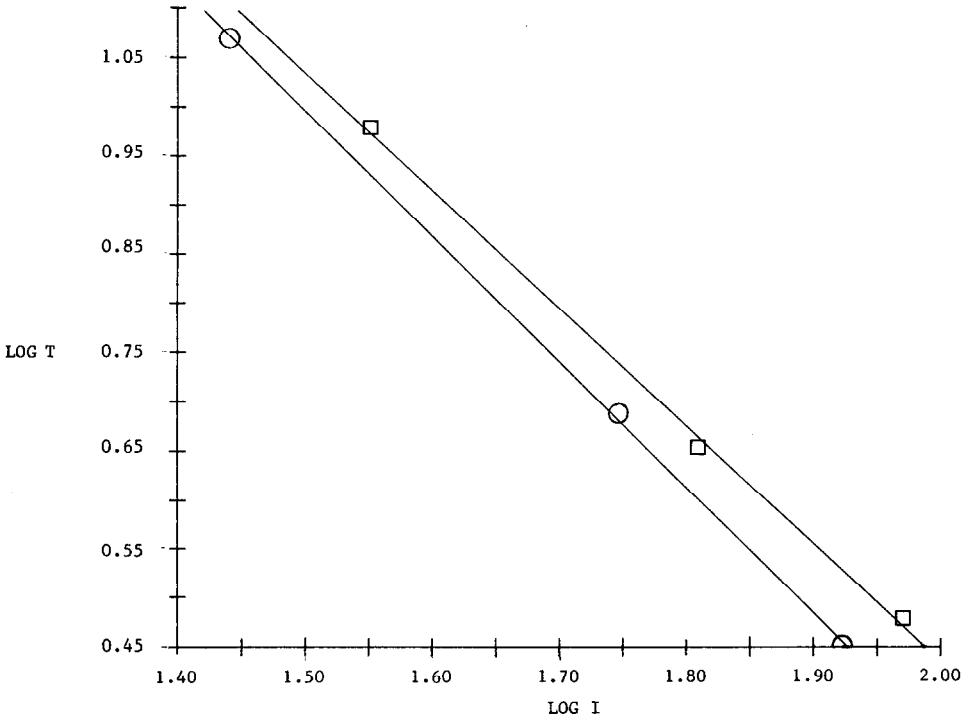

Fig. 1. Peukert plots of EV3000 (○) and Advanced (□) cells discharged at room temperature.

weight, 75 kg. At the 83 A rate, the mean specific energy for the 10 cells tested was 45.0 W h kg^{-1}. This compares with 41.5 W h kg^{-1} for the EV3000 at the same rate. The performance of the Advanced cell was very reproducible. The standard deviations for the average cell voltage and power were 0.6% of the mean, and for energy, 3.7%, at the 83 A rate.

The utilizations of the lead, lead dioxide and sulfuric acid for the EV3000 and Advanced cell designs are shown in Table 4 as a percentage of theoretical. The utilizations of the positive and negative active materials and

TABLE 4

Material utilization of EV3000 and Advanced cells

Design	Theoretical material utilization (%)			
	Discharge rate (A)	Positive	Negative	Acid
EV3000	83	31	46	56
Advanced	83	41	51	79
	94	37	46	72

the acid are 32, 11, and 41% higher, respectively, at the 83 A rate for the Advanced design compared with the EV3000. 83 A is the 3 h rate for the EV3000, whereas the 3 h rate for the Advanced cell is 94 A, because its capacity is higher. When the designs are compared at their respective 3 h rates, the material utilizations of the positive active material and the acid are 19 and 29% higher for the Advanced design, but the utilizations of the negative active material are about the same for the 2 designs.

At all rates the positive active material has the lowest utilization and the acid has the highest utilization. The lower utilization of the positive active material compared with the negative is due to the formation of water at the positive electrode, but not at the negative electrode, during discharge. This water dilutes the acid in the pores of the positive plate, causing increased polarization. The 79% acid utilization shown for the Advanced cell at 83 A is very close to the maximum practical limit. The discharge capacity is limited almost entirely by the total available acid and the acid concentration is reduced nearly to pure water in the pores of the positive electrode during discharge. Since the theoretical utilization, however, is based on the acid concentration used in these cells, it may still be possible to increase the energy density by increasing the acid concentration.

Cycle life data for an Advanced cell discharged at 83 A to a cutoff voltage of 1.75 V (100% depth of discharge) are shown in Fig. 2. Two cycles were run per day. Recharge was at a constant current of 48 A to a voltage limit of 2.5 - 2.65 V. Overcharge was controlled at 3 - 8%. Failure was

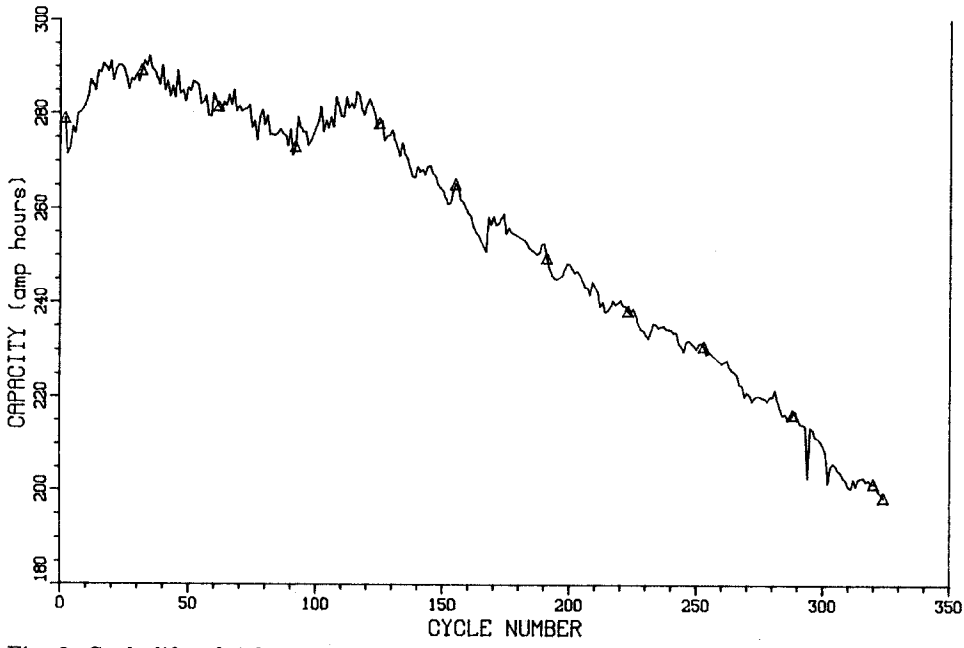

Fig. 2. Cycle life of Advanced cell cycled using an 83 A discharge rate to 1.75 V (100% depth of discharge).

defined as the point where the cell capacity declined to 200 A h. The cell cycled 325 times before reaching this capacity.

Failure modes of cycled cells were determined by (i) analyzing their electrochemical characteristics and (ii) by examining the quality of the positive and negative active materials. The positive active material was fractionated into shed, softened, and retained material. The shed material was collected from the bottom of the cell. The material left on the plates was rinsed with water to separate the softened material from that retained on the grid after the rinse. Plate materials were analyzed for lead, lead dioxide, lead sulfate, and antimony by wet methods. Surface areas were determined by BET.

The mode of failure appeared to be degradation of the active material in the positive plate. Grid corrosion was not severe. Cycle life tests on EV3000 cells indicated that the cycle life of cells at 80% depth of discharge is more than twice that at 100% depth of discharge when the failure mode is degradation of the positive active material [1]. If the same factor is applied to the Advanced design, a cycle life of more than 650 cycles at 80% depth of discharge can be projected.

The energy and coulombic efficiencies corresponding to the cycle life data in Fig. 2 are shown in Fig. 3 as a function of cycle number. Coulombic efficiencies of 92 - 97%, and energy efficiencies of 77 - 84% were achieved. These high efficiencies, which are similar to those of the ISOA designs [1], are due to the acid circulation subsystem.

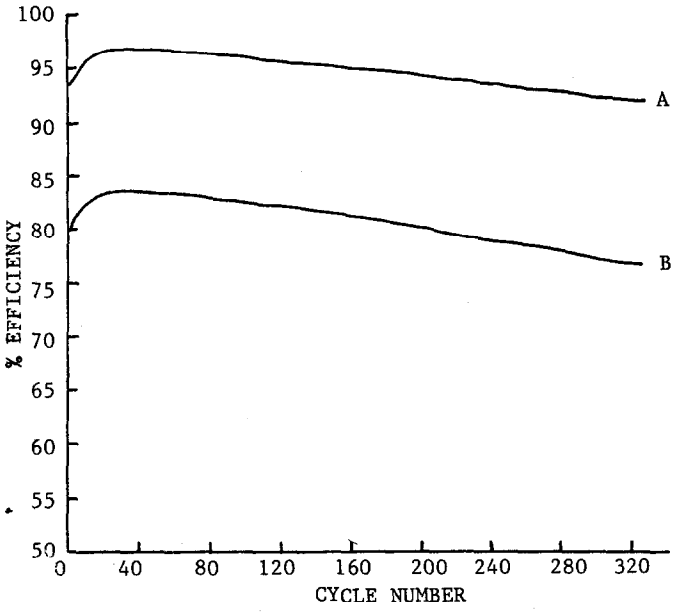

Fig. 3. % Coulombic (curve A) and energy (curve B) efficiencies as a function of cycle number for cell in Fig. 2.

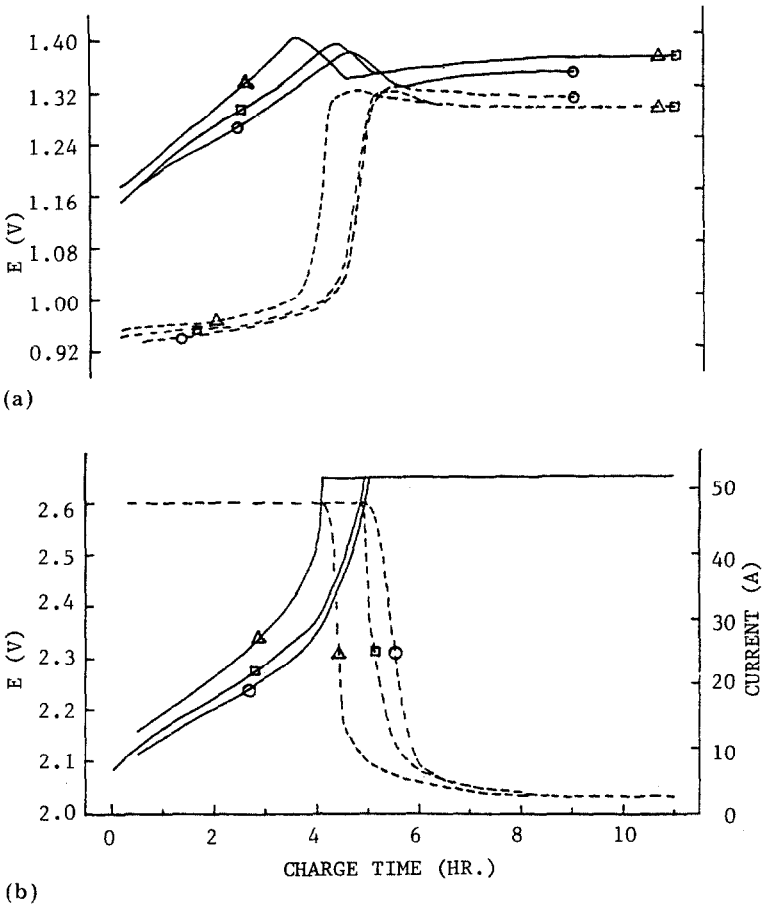

Fig. 4. Charging behavior of Advanced cell as a function of cycle number during 100% depth-of-discharge cycling. (a) Solid line is positive E; dashed line is negative E; (b) solid line is cell voltage; dashed line is current. O, Cycle 40; □, cycle 170; △, cycle 250.

The effect of cell aging on the charging behavior of the Advanced cell during 100% depth-of-discharge cycling is shown in Fig. 4. The total cell voltage, current, and half-cell potentials are given for cycles 40, 170 and 250. Table 5 presents the current acceptance as a function of charge voltage at cycles 170 and 270. As the cell ages, the onset of overcharge occurs earlier in the charge period, reflecting a reduction in the time needed to recharge the cell with declining discharge capacity. Although poisoning of the negative electrode by antimony migration has been reported previously [1] with increasing cycle number, it was not noticeable from the negative half-cell potential at the end of charge. The current acceptance was nearly constant between 170 and 270 cycles. The cell capacity remained positive limited throughout the cycle life.

TABLE 5

Current acceptance as a function of charge voltage

Cell voltage	Positive half cell voltage		Negative half cell voltage		Current acceptance (steady state) (A)	
(Cycles)	(170)	(270)	(170)	(270)	(170)	(270)
2.65	1.3653	1.3695	−1.2888	−1.2811	2.43	2.52
2.60	1.3460	1.3518	−1.2536	−1.2483	1.29	1.44
2.55	1.3308	1.3373	−1.2193	−1.2124	0.72	0.84
2.50	1.3209	1.3260	−1.1800	−1.1743	0.45	0.54
2.45	1.3168	1.3161	−1.1334	−1.1342	0.27	0.33

Acknowledgements

The help of our colleagues in Johnson Controls, Inc. Battery Engineering, and in particular of C. E. Weinlein, D. E. Bowman and E. N. Mrotek, is gratefully acknowledged. The leadership and helpful discussions of W. H. Tiedemann are also appreciated. J. L. Strebe and L. Y. Ellzey carried out the cell testing with care and diligence. The Johnson Controls, Inc. Materials Testing Laboratory performed the analyses of failed plate materials.

This work was supported by Johnson Controls, Inc. and by the Department of Energy under the direction of Argonne National Laboratory under Contract No. 31-109-38-4205.

References

1 K. R. Bullock, B. K. Mahato and G. H. Brilmyer, in K. R. Bullock and D. Pavlov (eds.), *Proc. Symp. on Advances in Lead–Acid Batteries, PV84-14*, The Electrochemical Soc., Inc., Princeton, NJ, 1984, p. 451.

2 E. N. Mrotek and P. J. Gurlusky, in M. A. Dorgham and J. M. Lafferty (eds.), *Technological Advances in Vehicle Design, Proceedings of the International Association for Vehicle Design, SP2*, Interscience Enterprises Ltd., UK, 1982, p. 116.

3 G. L. Wierschem, *Ext. Abstr., The Electrochem. Soc. Meet., Los Angeles, CA, October, 1979*, p. 249.

4 W. Peukert, *Electrotechn. Z, 18* (1897) 287.

5 R. M. Fiandt, *U.S. Pat. 3, 388, 007* (1968).

6 A. Sabatino and D. Orlando, *U. S. Pats. 3, 313, 658 (1967) and 3, 897, 269* (1975).

7 M. S. Baxa and C. E. Weinlein, *Ext. Abstr., The Electrochemical Soc. Meet., Detroit, MI, October, 1982*, p. 11.

8 J. R. Pierson and C. E. Weinlein, in J. Thompson (ed.), *Power Sources, 9*, Academic Press, London, 1983, p. 49.

9 W. Tiedemann, J. Newman and F. DeSua, in D. H. Collins (ed.), *Power Sources 6*, Academic Press, London, 1977, p.15.

10 G. L. Wierschem and W. H. Tiedemann, *Ext. Abstr., The Electrochem. Soc., Meet., Hollywood, FL, October, 1980*, p. 278.

11 D. Thuerk, paper presented at the *30th Power Sources Conf., Atlantic City, NJ, June, 1982.*

12 M. S. Inkmann, *U.S. Pat. 4, 221, 847*, Sept. 9, 1980.
13 C. E. Weinlein, paper presented at the *9th Energy Technol. Conf., Washington, DC, Feb., 1982.*
14 D. E. Bowman, in *Progress in Batteries and Solar Cells*, JEC Press, Cleveland, OH, 1984, p. 19.
15 B. L. McKinney, G. L. Wierschem and E. N. Mrotek, SAE Technical Paper Series, Paper No. 830229, Detroit, MI, 1983, in *Batteries for Electric Vehicles — Research, Development, Testing and Evaluation, Sp-541.*

BCI CYCLE LIFE TESTING PROCEDURES FOR DEEP-CYCLE LEAD–ACID BATTERIES

G. MAYER

Mellon Institute, Carnegie-Mellon University, Pittsburgh, PA 15213 (U.S.A.)